Endoplasmic reticulum stress induces tau pathology and forms a vicious cycle: Implication in Alzheimer's disease pathogenesis

Yuen-Shan Ho[1], Xifei Yang[1,5], Jeffery Chi-Fai Lau[1], Clara Hui-Ling Hung[1], Suthicha Wuwongse[1,4], Qishan Zhang[1], Jianzhi Wang[6], Larry Baum[7], Kwok-Fai So[1,2,3]

and Raymond Chuen-Chung Chang[1,2,3*]

[1]Laboratory of Neurodegenerative Diseases, Department of Anatomy, LKS Faculty of Medicine;

[2]Research Centre of Heart, Brain, Hormone and Healthy Aging;

[3]State Key Laboratory of Brain and Cognitive Sciences;

[4]Department of Psychiatry, LKS Faculty of Medicine;

The University of Hong Kong, Pokfulam, Hong Kong SAR, CHINA

[5]Shenzhen Centre of Disease Control and Prevention, Shenzhen, CHINA;

[6]Department of Pathophysiology, Tongji Medical College, Huazhong University of Science and Technology, Wuhan, CHINA

[7]School of Pharmacy, Faculty of Medicine, The Chinese University of Hong Kong, Shatin, Hong Kong SAR, CHINA

Running Title: ER-stress and tau pathology

Keywords: ER-stress; tau phosphorylation; thapsigargin; okadaic acid; Alzheimer's disease

***Correspondence address:**

Dr. Raymond C. C. Chang, Department of Anatomy, Faculty of Medicine, The University of Hong Kong, 21 Sassoon Road, Pokfulam, Hong Kong SAR, CHINA

Tel: (+852) 2819-9127; Fax: (+852) 2817-0857; E-mail: rccchang@hku.hk

Abstract

Accumulation of unfolded proteins can disturb the functions of the endoplasmic reticulum (ER), leading to ER-stress or unfolded protein responses (UPR). Recent data have shown that activation of UPR can be found in post-mortem brains of Alzheimer's disease (AD) patients; and biological markers for activation of UPR are abundant in neurons with diffuse phosphorylated tau. Although these observations suggest a linkage between ER-stress and tau pathology, little is known of their relationship. In this study, we found that high levels of phosphorylated PKR-like ER-resident kinase (p-PERK) and phosphorylated eukaryotic initiation factor 2 alpha (p-eIF2α) as markers for activation of UPR in the hippocampus of aged P301L mutant tau transgenic mice. The immunoreactivity of p-PERK was found to co-localize with that of phosphorylated tau. We then hypothesized that phosphorylation of tau could induce ER-stress and vice versa in promoting AD-like pathogenesis. By using the protein phosphatase 2A (PP2A) inhibitor okadaic acid (OA) as an inducer for phosphorylation of tau, we found that primary cultures of rat cortical neurons treated with OA triggered UPR as indicated by increased levels of p-PERK and p-eIF2α, splicing of mRNA for xbp-1 and elevated levels of mRNA for GADD153. On the other hand, thapsigargin (Tg) as an ER-stress inducer stimulated phosphorylation of tau at Thr231, Ser262 and Ser396. Tg also induced activation of caspase-3 and cleavage of tau. These findings suggested that ER-stress and hyperphosphorylation of tau could be induced by each other to form a vicious cycle to propagate AD-like neurodegeneration. (Word count: 246)

INTRODUCTION

Alzheimer's disease (AD) is an aging-associated neurodegenerative disease leading to progressive cognitive impairment and memory loss. Among various pathological changes in the development of AD, accumulation of senile plaques and neurofibrillary tangles (NTFs) has long been considered to be two distinct pathological hallmarks. Senile plaques are extracellular aggregates of β-amyloid (Aβ) protein; NTFs are intracellular filamentous inclusions which mainly consist of abnormally hyperphosphorylated and aggregated tau protein [1]. Both Aβ and tau are found in misfolded and aggregated forms in AD, suggesting that impairment of protein folding machinery is involved in the pathogenesis of AD.

In the eukaryotic cell, the endoplasmic reticulum (ER) is responsible for protein synthesis, correction of protein folding, post-translational modification and transport. In physiological circumstances, there is strict control of protein folding machinery, with misfolded proteins either retained in the ER for further correction of their folding or subjected to degradation [2]. Disturbance in the ER integrity or folding machinery by accumulation of misfolded proteins or changes of calcium homeostasis in the ER can trigger ER-stress responses, or the unfolded protein response (UPR) [3]. Shortly after perturbation of ER homeostasis, UPR can serve as an adaptation process to prevent further disturbance of cellular functions. Three ER-stress signaling pathways, including activation transcription factor 6 (ATF6), double-stranded RNA-dependent protein kinase (PKR)-like ER-resident kinase (PERK) and inositol requiring 1 (IRE1), are activated. These signaling cascades lead to increase production of ER-resident chaperones and foldases such as BiP/GRP78 to enhance efficiency of protein folding; the activation of eukaryotic initiation factor 2 alpha

(eIF2α) to shut down global protein translation for newly transcribed genes [4]; and the upregulation of ER-associated degradation to promote clearance of misfolded proteins [5]. Hence, UPR is considered to be initially protective.

However, sustained activation of the UPR can induce apoptotic responses that would finally cause cell death [6]. Although the involvement of ER-stress in neurodegenerative diseases such as AD and Parkinson's disease has been widely reported [7-9], the mechanisms by which ER-stress participates in neurodegenerative processes are not fully understood. Many studies reported the direct activation of both intrinsic and extrinsic apoptotic pathways by ER-stress [10-12]. Apart from apoptosis, it has also been suggested that ER-stress would alter cellular responses and sensitize neurons to Aβ toxicity, hence enhancing Aβ-induced neurodegeneration [13].

In postmortem AD brains, the levels of UPR markers such as BiP/GRP78 and p-PERK were found to be increased in the cortex and hippocampus [14,15], suggesting the involvement of ER-stress in AD pathogenesis. It is important to understand the role of ER-stress in the pathogenesis of AD and the related signaling pathways for the development of promising therapeutic interventions [16]. In familial AD (FAD), mutation of presenilin-1 (PS1) can alter signaling of UPR sensitizing neurons to be more vulnerable to stress. Mutant PS1 might increase the vulnerability of neurons to ER-Golgi toxin-induced apoptosis [17]; mutation of PS1 can also deregulate the expression of PERK, IRE1 and ATF-6 under ER-stress [8]. However, most AD cases are sporadic and lack PS1 mutations. As accumulation of aggregated Aβ and hyperphosphorylated tau have been considered to be the significant features in AD, it is reasonable to speculate that Aβ or tau are responsible for the induction of

ER-stress observed in AD. Previously, our laboratory had reported that extracellular accumulation of Aβ peptide in both fibrillar and oligomeric forms was not able to induce the UPR in primary cultures of cortical or hippocampal neurons [18,19]. In combination with the results showing that UPR was activated in pre-tangle neurons in AD brain [14], we speculated that hyperphosphorylated tau, instead of Aβ peptide, might play an important role in inducting ER-stress in AD. In the last two years, several studies had been conducted to investigate the effects of ER-stress on tau protein. The results, however, were controversial [14,20], and it is necessary to further clarify the relationship between ER-stress and tau.

In this study, we hypothesized that hyperphosphorylation of tau can induce ER-stress and vice versa in promoting pathogenesis of AD. Both transgenic mouse models and *in vitro* models were used to investigate the relationship between ER-stress and tau pathology. We found increased levels of p-PERK and p-eIF2α in the hippocampus of aged P301L mutant tau transgenic mice. Immunoreactivity of these two phospho-proteins co-localized with hyperphosphorylated tau. In primary cultures of cortical neurons, we observed that hyperphosphorylation of tau was induced by okadaic acid. Furthermore, we found that thapsigargin-induced ER-stress could trigger hyperphosphorylation as well as tau cleavage of tau. Our results suggested that hyperphosphorylation of tau and ER-stress can promote the initiation of each other and form a vicious cycle contributing to AD-like pathology.

MATERIAL AND METHODS

Materials and chemicals

Materials for cell culture, including minimum essential medium (MEM), Neurobasal™ medium, B-27 supplement, penicillin and streptomycin, were purchased from Gibco-BRL (Burlington, Ont., Canada). Other chemicals were obtained from the following companies: Thapsigargin (Tg) and okadaic acid (OA) were from Calbiochem, Inc. (La Jolla, CA, USA). 4-Phenyl butyric acid (4-PBA), protease inhibitor cocktail, phosphatase inhibitor cocktail, 4'6-Diamidino-2-phenylindole (DAPI), mouse monoclonal anti-β-actin antibody and mouse monoclonal anti-α-tubulin antibody were obtained from Sigma-Aldrich, Inc. (St. Louis, MO, USA). Mouse monoclonal antibody against cleaved-Tau (Asp421) was purchased from Upstate (Lake Placid, New York, USA). Rabbit polyclonal antibody against phosphorylated eIF2α (Ser51), tau pS396 against tau phosphorylated at Ser396, tau pT231 against tau phosphorylated at Thr231, tau pS262 against tau phosphorylated at Ser262 and mouse polyclonal antibody tau-1 against non-phosphorylated tau at Ser198/199/202 were purchased from BioSource International (Hopkinton, MA, USA). Horseradish peroxidase-conjugated goat anti-rabbit and goat anti-mouse antibodies were from DAKO (Glostrup, Denmark). Rabbit monoclonal antibody against phosphorylated PERK (Thr980), rabbit monoclonal antibody against total PERK, rabbit polyclonal antibody against anti-BiP, total eIF2α, phosphorylated-GSK3β (Ser9) and cleaved-caspase-3 were purchased from Cell Signaling Technology (Beverly, MA, USA). Mouse polyclonal antibody anti-GSK3β (pY216) to detect phosphorylated GSK3β at Tyr216, antibody Tau-5 to detect total tau and antibody against total GSK3β were from BD Transduction Laboratories (CA, USA). Polyvinylidene difluoride (PVDF) membrane was from Bio-Rad (Richmond, CA,

USA). Biomax X-ray film was from GE Healthcare (New York, USA). Enhanced chemiluminescence (ECL) detection kit was from Amersham (Buckinghamshire, UK). Anti-mouse or anti-rabbit Alexa fluor-488 or -568, Anti-Fade Gold mounting medium and Fluo-4AM were from Molecular Probes, Invitrogen. Anti-PHF-tau antibody clones AT180 against phosphorylated tau at Thr231 and Ser235 was from Thermo Scientific (Rockford, USA). Rabbit polyclonal antibody against human-tau (K9JA/ pan-tau, recognize the total tau at C-terminal part, amino acids 243–441) was from DAKO (USA).

Primary cultures of hippocampal and cortical neurons and drug treatment

Primary cultures of rat hippocampal and cortical neurons were prepared from embryonic day 17 Sprague-Dawley rat embryos (The Laboratory Animal Unit, The University of Hong Kong) via the method described previously [21,22]. Briefly, cerebral cortices or hippocampus were dissected in 1X phosphate-buffered saline (PBS) supplemented with glucose (18 mM). Neurons were then mechanically dissociated. Hippocampal neurons were seeded onto glass coverslips pre-coated with poly-L-lysine (25 μg/ml) at a density of 0.7×10^5 cells/coverslip. They were cultured with Neurobasal^{TM} medium containing 2% B-27, L-glutamine (2 mM), penicillin (50 U/ml) and streptomycin (50 μg/ml). Cortical neurons were seeded onto 6-well plates pre-coated with poly-L-lysine (25 μg/ml) at a density of 1.2×10^6 cells/well. They were cultured with minimum essential medium (MEM) supplemented with 5% heat inactivated fetal bovine serum, glucose (18 mM), L-glutamine (2 mM), insulin (5 μg/ml), progesterone (0.02 μM), putrescine (100 μM), selenium (30 pM), penicillin (50 U/ml) and streptomycin (50 μg/ml). All the neurons were maintained at conditions of 37°C in a humidified 5% CO_2 atmosphere. Deoxyfluorouridine (final concentration

1 μM) were added into cultures on DIV 2 to remove glial cells. All experiments were
2 performed on DIV 7.
3
4 To induce hyperphosphorylation of tau, the protein phosphatase 2A (PP2A)
5 inhibitor OA prepared as a 0.2 mM stock solution in DMSO was added into cultures
6 at a final concentration of 50 nM for the indicated duration. For control experiments,
7 DMSO was added at the final concentration present in the OA-treated cultures
8 (0.025%).
9
10 To induce ER-stress, Tg prepared as a 10 mM stock solution in DMSO was
11 added into cultures at final concentrations of 4 or 10 nM for the indicated duration.
12 For control experiments, DMSO was added at the final concentration present in the
13 Tg-treated cultures (0.0001%). In some experiments, the chemical chaperone 4-
14 phenyl butyric acid (PBA) 1 mM was added at the same time as Tg. The cultures were
15 then incubated for 6 h before they were harvested for Western blot analysis.
16
17 *Brain samples of transgenic mice expressing P301L human tau*
18 The transgenic mice (JNPL3 mice) expressing human mutant P301L tau
19 (proline to leucine mutation at amino acid 301 in exon 10) have been described
20 previously [23]. These $TgTau^{P301L}$ mice develop tau pathologies (tau
21 hyperphosphorylation and aggregation) starting from age 3-months and increasing in
22 severity with age [24]. Male wild type and $TgTau^{P301L}$ mice were sacrificed at age 21
23 months, and the brains were quickly excised and processed according to the following
24 procedures. For Western blot analysis, brains were micro-dissected for the
25 hippocampus and snap-frozen immediately in liquid nitrogen and stored at -80°C

before use. For histological and immunohistochemical analyses, all mouse brains were fixed with 0.1 M phosphate buffer (pH 7.6) containing 4% paraformaldehyde and embedded in paraffin. Each group contained at least 4 animals (n=4) for both immunohistochemical staining and Western blot analysis. In this study, we only focus on the hippocampus because it is the region mostly relevant to the development of AD, especially in the early stage. Since we did not keep the mice, other brain regions had been used by other investigators.

Immunohistochemical staining

For immunohistochemical analysis, consecutive 4-μm-thick coronal mouse brain sections were cut. After dewaxing and rehydration, the sections were treated with 0.01 M citrate buffer (pH 6.0) with 0.1% Tween-20 at 90°C for 15 min for antigen retrieval. The sections were then blocked with 10% normal goat serum in PBS for 1 h. Sections were co-incubated with primary antibody AT180 (1:200) and phosphorylated-PERK (1:200) at 4°C overnight. After washing with PBS, the sections were stained with secondary antibody, Alexa fluor-488 or -568 for 2 h and finally stained with DAPI for revealing the nuclei. Sections were then mounted with Anti-Fade Gold mounting medium. The sections were examined with a BioRad Radiance 2100 confocal microscopic system.

Western blot analysis

Total lysate was collected from cell culture or mouse brain samples as described elsewhere [25]. In brief, cultured neurons or brain samples were lysed in ice-cold lysis buffer (10 mM Tris-HCl (pH 7.4), 1 mM NaCl, 20 mM $Na_4P_2O_7$, 2 mM Na_3VO_4, 1% Triton-X-100, 10% glycerol, 0.5% deoxycholate, 0.1% SDS, 1 mM

phenylmethylsulfonyl fluoride, protease inhibitor cocktail and phosphatase inhibitor cocktail). After homogenization and centrifugation, the supernatant was collected. The sample were subjected to SDS 10% or 12.5% polyacrylamide gels electrophoresis and transferred to PVDF membranes. Membranes were blocked with 5% w/v non-fat milk in TBST (TBS containing 0.1% Tween-20) for 1 h to prevent non-specific binding. Primary antibodies were diluted in TBST and incubated with the membrane as described follow: cleaved caspase-3 (1:2000), cleaved-tau (Asp421) (1:1000), tau pS396 (1:4000), tau pT231 (1:4000), tau pS262 (1:2000), tau-1 (1:30,000), pan-tau (1:4000), phosphorylated PERK (1:1000), total PERK (1:1000), phosphorylated eIF2α (1:1000), total eIF2α (1:2000), BiP (1:1000), p35/p25 (1:2000), CDK5 (1:2000), p-GSK3β (Ser9) (1:4000), p-GSK3β (pY216) (1:6000). After washing, the membranes were incubated with horseradish peroxidase-conjugated secondary antibodies (1:2000) for 1 h and subsequently developed by using the ECL or ECL-plus Western blotting detection kit. The membranes were then stripped with stripping buffer (50 mM glycine, 2% SDS, pH 2.0) and re-probed with monoclonal anti-β-actin antibody (1:10,000, 1 h) and goat anti-mouse HRP secondary antibody. Optical density of the blots was measured with Image J software (National Institutes of Health, USA).

Analysis of splicing in x-box binding protein (*xbp-1) mRNA*

Splicing in xbp-1 mRNA was investigated by RT-PCR and PstI restriction enzyme digestion as in our previous studies [18,19]. After treatment with OA, extraction of RNA and reverse transcription were carried out. cDNA of Xbp-1 was amplified using PCR (Invitrogen) with xbp-1 specific primers (Table 1) in a RoboCycler 96 (Stratagene). The PCR cycles consisted of denaturation at 94^{o}C for 1

min, annealing at 62°C for 1 min and extension at 72°C for 1 min, for 33 cycles. PstI (New England Biolabs) restriction digestion of the 600 bp PCR products was done at 37°C for 16 h. The restriction fragments were separated on a 1% (w/v) agarose gel with ethidium bromide and visualized under UV illumination.

Reverse Transcription (RT)-PCR

After exposure to OA [50 nM] for different times, total RNA from neurons was extracted with NucleoSpin® RNA II (Macherey-Nagel, Germany). Total RNA yields were measured by A260/280 using GenQuant II (Pharmacia Biotech). 1 μg RNA was reverse-transcribed into cDNA with Superscript™ III first strand synthesis system (Invitrogen) for RT-PCR. PCR was done in a RoboCycler 96 (Stratagene) with *Taq* polymerase (Invitrogen). Target genes for amplification and their primer sets and thermal conditions are listed in Table 1.

Measurement of intracellular free calcium concentration ($[Ca^{2+}]_i$)

Cultured cortical neurons were incubated with Fluo-4AM [1 μM] in cell culture medium as indicated above for 30 min at 37°C. After incubation, the loading medium was removed, and cells were washed with 1X HBSS and maintained in 0.5 ml of the same solution in dark. The fluorescence signals were recorded at 488 nm (excitation wavelength) and 538 nm (emission wavelength) with a Bio-Rad Radian 2100 confocal microscope system. Upon measurement, the first 120 s were recorded to serve as the baseline of $[Ca^{2+}]_i$ before any drug application. At 120 s, Tg was added into the culture dish to a final concentration of 10 nM or 20 μM. The $[Ca^{2+}]_i$ was recorded for another 400 s. At least 4 independent experiments were performed, and the readings of 9 neurons were recorded from each individual experiment. Data were

represented as fold of control [fold of control was calculated as follows = reading at particular time point/ mean of reading of baseline].

Statistical analysis

Data were expressed as mean ± standard error (SE) from at least 3 independent experiments. The significance of the differences among different groups was determined by unpaired *t*-test or one-way ANOVA, followed by Student Newman-Keuls as post-hoc test. $P < 0.05$ was considered to be statistically significant.

Results

Increased levels of UPR markers were observed in the hippocampus of aged P301L tau transgenic mice

In postmortem AD brains, immunoreactivity of p-PERK was found to be increased and associated with phosphorylated tau [14]. To explore the relationship between ER-stress and tau pathology, we examined the levels of p-eIF2α and p-PERK in 21-month-old $TgTau^{P301L}$ mice. Levels of p-eIF2α in hippocampus of $TgTau^{P301L}$ mice were 3.2 ± 0.4 fold those of age-matched controls (Fig. 1A). Activation (phosphorylation) of eIF2α can lead to inhibition of protein translation, and eIF2α can be phosphorylated by up-stream kinases such as double-stranded RNA-dependent protein kinase (PKR), PERK, amino acids-regulated eIF2α kinase (GCN2) or heme-regulated eIF2α kinase (HRI) [26]. Among these kinases, the role of PERK during ER-stress has been well-reported; therefore, we further examined the immunoreactivity of p-PERK in brain sections of these transgenic mice. We found that the immunoreactivity of p-PERK was markedly increased in the hippocampus of $TgTau^{P301L}$ mice compared to age-matched controls. Furthermore, the elevated immunoreactivities of p-PERK were found to be co-localized with AT180 immunoreactivity, which detects tau phosphorylated at Thr231 and Ser235 (Fig. 1B). Thus, ER-stress was increased in aged $TgTau^{P301L}$ mice.

Induction of tau hyperphosphorylation led to ER-stress in primary cultures of cortical neurons

In the previous section, we had demonstrated that aged $TgTau^{P301L}$ mice had increased levels of p-PERK, which was co-localized with AT180 staining. Our results suggested that there might be a direct linkage between phosphorylation of tau and ER-

stress. We then asked whether the UPR was induced by hyperphosphorylation of tau. OA is a well-reported inducer for hyperphosphorylation of tau; it acts by inhibiting protein phosphatase 2A (PP2A) that is responsible for dephosphorylation of tau [27,28]. OA was applied to primary cultures of cortical neurons to induce hyperphosphorylation of tau. As shown in Fig. 2A-E, 50 nM OA induced the hyperphosphorylaton of tau on Thr231, Ser396 and Ser198/199/202 at different time points. Except for phosphorylated tau at Ser396, which decreased after 16 h, the other phosphorylation sites of tau showed persistent increases in their immunoreactivity. It had been reported that changes in some tau epitopes induced by OA were more persistent than others; hence our results were consistent with previous findings [29]. The level of total tau (as detected by the Tau-5 and K9JA antibodies) was decreased in neurons exposed to OA (Fig. 2A and Supplementary Fig. 3A), which has been previously reported by another group [30]. It has been speculated that the reduction in total tau indicates either an enhanced clearance of aggregated tau (due to hyperphosphorylation) or an ineffectiveness of detection for aggregated tau by Western blot analysis. Nevertheless, OA clearly induced hyperphosphorylation of tau. To further confirm our observation, we performed immunocytochemical staining on primary cultures of hippocampal neurons; and we found that OA could also induce tau hyperphosphorylation in these cells (Supplementary Fig.1). Since we observed similar phenomenon between the two cell types, and there were limited availability of primary hippocampal neurons, we used cortical neurons for most of our experiments.

We then detected the presence of ER-stress by OA. We found that immunoreactivity of p-PERK significantly increased from 6 to 24 h while that of p-eIF2α exhibited a tendency toward an increase at all time-points (though statistically significance was only detected at 24 h) (Fig. 2F, G, I). The level of BiP was

unchanged at all tested time-points. To further confirm the presence of UPR in neurons after treatment of OA, we detected splicing of mRNA for xbp1 and the mRNA level of GADD153 (growth arrest-and DNA damage-inducible gene 153). UPR activates IRE1 to function as an endoribonuclease to splice mRNA for xbp-1 by cutting off a 26-nucleotide intron [31]. This would prevent the digestion of mRNA for xbp-1 (~600bp) by Pst1 as the Pst1 restriction enzyme cutting site is within the excised 26-nucleotide sequence. Fig. 2J shows that it was about 600 bp of mRNA for xbp-1 before Pst1 digestion in all treatment groups. After Pst1 digestion (Fig. 2K), fragments of about 300 bp were only found in controls. In neurons exposed to OA for 16 or 24 h or to DTT [1mM] for 24 h (a positive control), the digestion of xbp-1 by Pst1 to yield a 300 bp fragment was attenuated, indicating the splicing of mRNA for xbp-1. Our results suggested that OA induced UPR and activation of IRE1. GADD153 is a highly inducible gene responsive to ER-stress; its expression increases during UPR [32]. As shown in Fig. 2L, the level of mRNA for GADD153 significantly increased after exposure of neurons to OA for 16 and 24 h. Taken together, our data showed that OA-induced hyperphosphorylation of tau could trigger UPR.

Induction of ER-stress by thapsigargin led to increased phosphorylation of tau in primary cultures of cortical neurons

Our *in vivo* and *in vitro* data suggested that hyperphosphorylation of tau could induce ER-stress. It has well been reported that prolonged ER-stress can lead to apoptosis. Besides inducing neuronal cell death as late and final events, ER-stress may also induce other pathological changes which are involved in the neurodegenerative process of AD. We, therefore, examined the effects of thapsigargin

(Tg) as a typical ER-stress inducer on an *in vitro* model of primary cultures of cortical neurons. Tg is a specific inhibitor of intracellular Ca^{2+}-transport ATPases. It blocks the activity of the enzyme to induce perturbation of intracellular calcium homeostasis, resulting in ER-stress. As shown in Fig. 3A-D, 10 nM Tg induced an elevation of immunoreactivities of UPR markers including p-PERK and BiP in a dose-dependent manner. We then detected the levels of phosphorylated tau. The band intensity of phosphorylated tau at Thr231, Ser262 and Ser396 was found to increase at 6 and 12 h time points (Fig. 3E-H). These elevated immunoreactivities of phosphorylated tau were then reduced at 18 h and became similar to levels of the controls. The immunoreactivity of phosphorylated tau (Thr231 and Ser396) continued to decrease and became markedly lower than the controls at 24 h (Fig. 3F and H). The immunoreactivity of Tau-5 and K9JA (both detected total tau level) among all the treatment groups was similar without significant change,

Truncation of tau was induced by ER-stress

It has been reported that Tg-induced ER-stress can lead to activation of caspase-3 and apoptosis [33]. Tau is a substrate of caspase-3, and its cleaved form is pro-apoptotic [34] and is more prone to form aggregates [35]. We therefore examined the levels of caspase-3 and cleaved tau in our Tg-treated cortical neurons. We found that the immunoreactivity of cleaved caspase-3 showed a trend toward increase after 12 h exposure to 10 nM Tg. After 18 or 24 h incubation, the immunoreactivity of cleaved caspase-3 significantly increased to nearly 3-fold of the control. The increase also showed a dose-dependent pattern. At the same time, the immunoreactivity of cleaved-tau at Asp421 was also elevated in a pattern similar to that of caspase-3 (Fig.

4). At 18 h, the immunoreactivity of cleaved-tau reached the highest levels and was more than 7-fold greater than the control (Fig. 4B).

Induction of tau phosphorylation by Tg [10 nM] was due to the accumulation of misfolded/unfolded protein

To confirm whether Tg-induced hyperphosphorylation of tau was a result of UPR, we co-treated cortical neurons with Tg and 4-phenyl butyric acid (4-PBA), a chemical chaperone which can enhance the adaptive capacity of the ER [36]. As shown in Fig. 5A-D, 1 mM 4-PBA significantly reduced the immunoreactivity of phosphorylated tau induced by Tg. There was little effect of 4-PBA itself on immunoreactivities of phosphorylated tau at Thr231 and Ser 262, but 4-PBA did increase the immunoreactivity of phosphorylated tau at Ser396. Our results confirmed the role of ER-stress in Tg-induced tau phosphorylation.

Exposure of cortical neurons to Tg [10 nM] did not induce acute increase of $[Ca^{2+}]_i$

Tg can disturb intracellular calcium homeostasis and cause a transient increase in $[Ca^{2+}]_i$ [37]. Previous study has shown that a transient increase in $[Ca^{2+}]_i$ can result in prolonged phosphorylation of some tau epitopes [38]. To investigate the downstream causative factors that mediated phosphorylation of tau in our Tg-treated cultures, we measured the levels of $[Ca^{2+}]_i$. Our data showed that 10 nM Tg did not trigger an acute and transient increase in $[Ca^{2+}]_i$. There was a mild increase in $[Ca^{2+}]_i$ only for 1.06 ± 0.02 fold of control. There were only gradual changes in $[Ca^{2+}]_i$ induced by 10 nM Tg. As a positive control, we also treated cortical neurons with 20 μM Tg, and we found that this concentration of Tg could induce a 1.43 ± 0.08 fold increase in $[Ca^{2+}]_i$. As shown in Fig. 6, 20 μM Tg induced a typical calcium influx

pattern, in which $[Ca^{2+}]_i$ increased immediately after loading of Tg, peaked at about 240 s, then decreased gradually.

Tg did not induce significant change in the level of p-GSK3β

To investigate possible upstream kinases affected by ER-stress and tau phosphorylation, we detected the levels of p-GSK3β, by Western-blot analysis (Fig. 7A). GSK-3β can be activated by dephosphorylation at Ser 9 or phosphorylation at Tyr 216. We found that the immunoreactivity of p-GSK3β (Ser9) showed a trend toward increase at 6 h and remained the same as the controls at other detected time points (Fig. 7B). The immunoreactivity of p-GSK3β (pY216) remained the same as that of the controls at all detected time points (Fig. 7C). There was no significant change in the protein levels of total GSK3β (data not shown).

Discussion

ER-stress can trigger UPR, which is an adaptive response to cope with the accumulation of misfolded proteins. It is believed that ER-stress is linked to a number of neurodegenerative diseases including AD [3]. In postmortem AD brain, activation of the UPR was found in neurons with diffuse phosphorylated tau [14,15]; yet the temporal sequence of the events is not clear. Our study aims to investigate the causative relationship between ER-stress and phosphorylation of tau. By using three models, both *in vivo* and *in vitro*, we provide evidence that ER-stress and tau phosphorylation are closely linked.

Our initial hypothesis is to prove that abnormal tau can lead to ER-stress and activation of UPR. To study the chronic effects of tau pathology on ER-stress, transgenic mice which display phosphorylated and aggregated tau would be an appropriate experimental model as they can mimic the chronic disease development process. The first model we used was therefore aged $TgTau^{P301L}$ transgenic mice. These mice expressed the P301L mutant version of the longest form of human tau (4R0N), which can cause frontotemporal lobe dementia with parkinsonism linked to chromosome 17 (FTDP-17). They developed pre-tangles and NFTs with increasing age [23]. Tau pathology can be observed in different regions of the P301L mice including the cortex, hippocampus, midbrain and cerebellum. Since we only focused on the hippocampus in this study, we are not sure if similar phenomenon on ER stress can be observed in other regions. The change of cognitive functions in P301L mice has been studied by other groups. Although there was a report showing normal cognitive function of these mice [39], another study found that these mice had poorer cognitive performance, which was associated with increased number of

phosphorylated tau containing neurons in cerebral cortex and hippocampus [40]. Another group also reported that the P301L mice showed decline in cognitive functions evaluated by Morris-water maze test [41]. Hence, TgTau^{P301L} transgenic mice can be an appropriate animal model for studying tau pathology related to ER-stress. In view of all these published behavioral reports of cognitive functions of this line of mice, our study mainly focused on the pathological changes in these mice rather than the behavioral functions. We therefore did not perform cognitive function tests. Our data showed that the levels of p-PERK were elevated in the hippocampus of aged TgTau^{P301L} mice, and the staining was co-localized with phosphorylated tau. The levels of p-eIF2α were also increased in the hippocampus of these transgenic mice. Our data have proved that ER-stress and UPR occur in aged TgTau^{P301L} mice; and hence ER-stress and tau pathology might have a casual relationship. In fact, a previous report showed that the amount of tau protein was preferentially increased in the membrane of the rough ER in motor neurons of TgTau^{P301L} mice; and hyperphosphorylated tau was associated with the ER membrane in AD brains [42]. These findings further support the notion that abnormal tau would affect ER function in the neurodegenerative process. Interestingly, another research group has reported recently that they could not find any evidence of ER-stress or UPR activation in another mutant tau transgenic mice model [20]. In that study, transgenic mice expressing the P301S mutant version of human tau (PS19 transgenic mice) were used. These PS19 transgenic mice gradually developed synaptic loss, neuronal loss and NFTs with increasing age [43]. The reason for the opposite results observed in these two transgenic models is unclear. One may question that the elevation of ER-stress markers in our model may be due to the specific mutant i.e. P301L. Since we do not have the htau mice which overexpress human wild-type tau, we cannot examine the

levels of ER-stress in these animals to exclude the possibility. In this study, the use of $TgTau^{P301L}$ mice only serve as an model to show that tau phosphorylation is correlated to ER-stress, and we are not intend to use it as an experimental model of AD.

With the results in transgenic animals, it is better to further study the mechanisms in vitro. We further prove that phosphorylation of tau can lead to ER-stress in an *in vitro* model. Previous findings reported by Kim et al. have shown that OA induced the phosphorylation of eIF2α; and hence the translocation of activating transcription factor (ATF4) and induction of apoptosis [44]. Our present study further proved the involvement of ER-stress in OA-induced phosphorylation of tau. Our preliminary data showed that phosphorylation of tau occurs as early as 1 h after OA treatment, while the levels of p-eIF2α also increased as early as 1 h. It is known that eIF2α can be phosphorylated under many situations, and its phosphorylation alone is insufficient to prove the presence of ER-stress. Here we reported that, after OA treatment, elevation of the levels of p-PERK was observed only after 6 h; splicing of mRNA for xbp-1 and increased expression of mRNA for GADD153 were observed only at late time points (16 and 24 h). These findings clearly demonstrated activation of the PERK and IRE1 pathways in the UPR; and more importantly, the occurrence of the UPR follows the phosphorylation of tau, suggesting a causal relationship between the two factors. In the later time points i.e. 16 h and 24 h, the levels of phosphorylated tau at Ser 396 decreased (Fig. 2A). Although we did not study the apoptotic signal or apoptotic state in OA-treated neurons as it is not our aim of study, previous report documented that treatment with OA leads to apoptosis in late time points [45]. This decrease in tau phosphorylation may be explained by the entrance of the early phase of apoptosis [46]. It was shown that when neurons were exposed to stress factors such

as staurosporine, tau was first hyperphosphorylated transiently and then undergone dephosphorylation and cleavage, followed by apoptosis [47]. We speculate that under OA-treatment, tau may also be dephosphorylated when neurons undergo apoptosis.

While phosphorylation of tau can induce UPR, induction of ER-stress has been shown to induce phosphorylation of tau. Tg was used to induce ER-stress in our study. In many studies [48,49], high concentrations of Tg at micromolar levels were used to induce ER-stress and apoptosis. Since we aimed to examine the events that occur before the induction of apoptosis, we chose a very low dose of Tg (10 nM) to induce ER-stress. It has been shown that treatment of primary cultures of cortical neurons with Tg [10 nM] for 24 h did not affect cell viability, and significant cell death was observed at 48 h [48]. We demonstrated here that this low concentration of Tg could induce the UPR as early as 6 h; and at the same time, there was a transient increase in the phosphorylation of tau. Interestingly, when we investigated the kinases that may be responsible for Tg-induced tau phosphorylation, we found that GSK3β was unlikely to be involved. The levels of p-GSK-3β (Ser9), which is the inactivated form, were even increased after Tg treatment. This contradicts to a recent report suggesting that Tg-induced phosphorylation of tau could be attenuated by inhibiting activity of GSK3β [50]. Since we used primary cultures of cortical neurons as our model system, while they used a neuronal cell line and animals in their study, it is difficult to have a direct comparison between the results. Another possibility for causing the discrepancy would be the dosage of Tg in the experiments. The concentration of Tg in our study was very low. As shown in Fig. 6, 10 nM Tg did not induce even a sharp and transient increase in $[Ca^{2+}]_i$, yet this dosage of Tg was sufficient to induce ER-stress as shown in Fig. 3. It has been shown that Tg at even

subnanomolar concentration is effective at inhibiting Ca^{2+}-ATPase [51]. Our data suggested that tau was very sensitive to environmental stress, and post-translational modification of tau can be altered by a slight change in intracellular homeostasis. In Tg-treated neurons, apart from phosphorylation, truncation of tau was also observed together with activation of caspase-3 at late time points (Fig. 4). Caspase-cleaved tau in immortalized cortical neurons was found to increase neuronal susceptibility to ER-stress [52]. Hence, it is possible that the cleaved tau generated after treatment of Tg can further promote UPR leading to neurodegeneration. It is worth to note that in the late time points (18 and 24 h), the levels of UPR markers continued to increase while that of phosphorylated-tau decreased. Under the exposure of Tg, it is not surprised that ER-stress response would continue in the later time points. The prolonged ER-stress displayed activated caspase-3, the observed tau dephosphorylation and cleavage may therefore represent the entrance of the execution phase of apoptosis [53]. Since the phosphorylation of tau can be affected by multiple factors during prolonged stress, this makes it more difficult to observe the causal relation between ER stress and tau hyperphosphorylation. Nevertheless, we showed that the chemical chaperone 4-PBA reduced the levels of phosphorylated-tau in Tg-treated neurons in early time point (6 h). This gives evidence that the level of ER stress is correlated to the changes of phoshorylated tau.

While GSK3β is unlikely to be involved in Tg-induced phosphorylation of tau in our system, we also detected other possible candidates involved in this process. We found that there were no changes in the levels of p-PP2A (Tyr 307) (data not shown); but there were dose-dependent decreases in levels of p35, suggesting the possible involvement of CDK5 (data not shown). Since we did not find a clear increased level of p25, which is a critical factor for activation of CDK5, the role of CDK5 in Tg-

induced tau pathology will be further investigated. Previous findings suggested that dysregulation of CDK5 is involved in ER-stress mediated apoptosis [54]. Nevertheless, detailed mechanistic linkage between ER-stress and phosphorylation of tau in relation to CDK5 will be further examined.

Our findings provide evidence showing that ER-stress and phosphorylation of tau can induce each other. We propose that ER-stress can play an important role in AD-like pathogenesis since ER-stress can induce phosphorylation of tau and form a vicious cycle. This close relationship between ER-stress and tau pathology might be one of the common pathways to explain the multi-factorial nature of AD. Many risk factors for AD are found to be associated with ER-stress. For example, prolonged light illumination of mice to deprive them of sleep has been shown to induce AD-like pathology and ER-stress [55]; hyperhomocysteinemia and stroke can induce ER-stress [13,56,57]. Abnormal phosphorylation of tau is always found in these situations [21,55,58,59]. Given that the consequence of ER-stress responses will be translated into hyperphosphorylation of tau protein, and ER-stress is very sensitive to environmental changes (even without perturbation of ER calcium, as demonstrated in our study), it is therefore understandable that phosphorylation of tau was observed in different pathological conditions. Understanding the role of ER-stress and its relationship with tau protein would certainly aid the development of promising therapeutic interventions for AD.

Acknowledgement

This work is supported by the HKU Alzheimer's Disease Research Network, Azalea (1972) Endowment Fund, General Research Grant (755206M & 761609M), NSFC/RGC Joint Research Scheme (N_HKU707/07M) from Research Grant Council and HKU Seed Funding for Basic Science Research (200911159082) to RCCC. CHLH, SW and QSZ are supported by the Graduate School; YSH is supported by a Postdoctoral Fellowship, The University of Hong Kong.

Figure legends

Fig. 1 Increased levels of markers for UPR and hyperphosphorylation of tau were observed in the hippocampus of aged TgTau^{P301L} mice. (A) Western blots show the levels of p-eIF2α and total eIF2α in the hippocampi of 21-month-old TgTau^{P301L} mice and age-matched wild type mice (upper panel). Quantitative analysis of the immunoreactivity of p-eIF2α / total eIF2α was performed by Image J (lower panel). Data represent mean ± SE from at least 3 independent experiments. Statistical analysis was performed by unpaired *t*-test. *$p<0.05$ compared to WT mice. (B) AT180 and p-PERK staining of the hippocampi of 21-month-old TgTau^{P301L} mice and age-matched wild type mice. CA3 region is shown in the photos (40X). There was little staining of AT180 in WT mice, but AT180 immunoreactivity increased markedly in the TgTau^{P301L} mice and was colocalized with p-PERK immunoreactivity.

Fig. 2 OA-induced hyperphosphorylation of tau led to ER-stress in primary cultures of cortical neurons. Neurons were exposed to OA [50 nM] for 6, 16 or 24 h. (A to E) The levels of total tau and p-Tau at Thr231, Ser262, and Ser198/199/202 were detected by Western blot analysis. (F to I) The levels of p-PERK, total PERK, p-eIF2α and total eIF2α were detected by Western blot analysis. β-Actin was used as internal control. Quantitative analysis of the immunoreactivity of the detected proteins was performed by Image J. Data represent mean ± SE from at least 3 independent experiments. Statistical analysis was performed by unpaired *t*-test. (J) RT-PCR was performed to amplify mRNA for xbp-1, (K) followed by Pst1 restriction enzyme digestion. DTT [1mM] served as a positive control to induce alternative splicing in mRNA for xbp-1, as shown by the absence of ~300 bp digestion fragment after Pst1 restriction enzyme digestion. (L) Levels of mRNA for GADD153 were detected by

PCR. Photos of agarose gel electrophoresis are representatives from three independent experiments. (M) Quantitative analysis of the mRNA levels for GADD153 was performed by Image J. Data represent mean ± SE from at least 3 independent experiments. Statistical analysis was performed by unpaired *t*-test. *$p<0.05$ compared to corresponding control.

Fig. 3 Tg induced UPR and phosphorylation of tau in primary cultures of cortical neurons. Tg [4 or 10 nM] was added to neuronal cultures and incubated for different durations to induce ER-stress. (A to D) The levels of UPR markers including p-PERK, BiP/GRP78, and p-eIF2α were detected by Western blot analysis. (E to H) The levels of total tau and p-tau at Thr231, Ser262 and Ser396 at different time-points were detected. α-Tubulin was used as internal control. Quantitative analysis of the immunoreactivity was performed by Image J. Data represent mean ± SE from at least 3 independent experiments. Statistical analysis was performed by one-way ANOVA for multiple comparisons, followed by Student Newman-Keuls as post-hoc test. *$p<0.05$ compared to corresponding control.

Fig. 4 Tg induced activation of caspase-3 and truncation of tau. Tg [4 or 10 nM] was added into neuronal cultures and incubated for different durations to induce ER-stress. (A) The levels of cleaved tau and cleaved caspase-3 were detected by Western blot analysis. α-Tubulin was used as internal control. Quantitative analysis of the immunoreactivity was performed, and the results are shown in (B and C). Data represent mean ± SE from at least 3 independent experiments. Statistical analysis was performed by one-way ANOVA for multiple comparisons, followed by Student Newman-Keuls as post-hoc test. *$p<0.05$ compared to corresponding control.

Fig. 5 Tg-induced phosphorylation of tau was attenuated by the molecular chaperone 4-PBA. Primary cultures of cortical neurons were co-treated with 4-PBA [1 mM] and Tg [10 nM] for 6 h. (A) Total cell lysates were collected for the detection of p-tau at Thr231, Ser262 and Ser396. Representative images of Western blot films were shown. (B to D) Quantitative analysis of the immunoreactivity was performed, and the results were shown. Data represent mean ± SE from at least 3 independent experiments. Statistical analysis was performed by one-way ANOVA for multiple comparisons, followed by Student Newman-Keuls as post-hoc test. #$p<0.05$ compared to control. *$p<0.05$ compared to cultures treated with Tg [10 nM].

Fig. 6 Tg [10 nM] did not trigger an acute elevation of $[Ca^{2+}]_i$. Tg-induced changes in $[Ca^{2+}]_i$ were detected by using Fluo-4AM dye. Cortical neurons were exposed to Tg [10 nM or 20 μM] at time 120 s. The changes of $[Ca^{2+}]_i$ were detected and expressed as fold of control. Data represent mean ± SE from at least 4 independent experiments.

Fig. 7 Tg did not induce activation of GSK3β but induced the cleavage of p35. Primary cultures of cortical neurons were incubated with Tg [4 or 10 nM] for different durations. (A) Total cell lysates were collected for the detection of p-GSK3β (Ser9) and p-GSK3β (pY216) by Western blot analysis. α-Tubulin was used as internal control. (B and C) Quantitative analysis of the immunoreactivity was performed. Data represent mean ± SE from at least 3 independent experiments. Statistical analysis was performed by one-way ANOVA for multiple comparisons, followed by Student Newman-Keuls as post-hoc test. *$p<0.05$ compared to corresponding control.

Table 1

Primer sequences and reaction conditions for RT-PCR

Target genes	Sequence	Product size (bp)	Annealing temperature (^{o}C)	No. of cycles
GAPDH	F: 5'- gcaagttcaacggcacag-3' R: 5'- gccgtagactccacgacat-3'	140	62	33
Xbp-1	F: 5'-aaacagagtagcagcgcagactgc-3' R: 5'-ggatctctaaaactagaggcttggtg-3'	600	62	33
GADD153	F: 5'-tcagatgaaattgggggcac-3' R: 5'-tttcctcgttgagccgctcg-3'	340	60	35

REFERENCES

[1] Querfurth HW, LaFerla FM (2010) Alzheimer's disease. *N Engl J Med* **362**, 329-344.

[2] Schroder M , Kaufman RJ (2005) ER stress and the unfolded protein response. *Mutat Res* **569**, 29-63.

[3] Lindholm D, Wootz H, Korhonen L (2006) ER stress and neurodegenerative diseases. *Cell Death Differ* **13**, 385-392.

[4] Harding HP, Zhang Y, Ron D (1999) Protein translation and folding are coupled by an endoplasmic-reticulum-resident kinase. *Nature* **397**, 271-274.

[5] Friedlander R, Jarosch E, Urban J, Volkwein C, Sommer T (2000) A regulatory link between ER-associated protein degradation and the unfolded-protein response. *Nat Cell Biol* **2**, 379-384.

[6] Marciniak SJ, Ron D (2006) Endoplasmic reticulum stress signaling in disease. *Physiol Rev* **86**, 1133-1149.

[7] Milhavet O, Martindale JL, Camandola S, Chan SL, Gary DS, Cheng A, Holbrook NJ, Mattson MP (2002) Involvement of Gadd153 in the pathogenic action of presenilin-1 mutations. *J Neurochem* **83**, 673-681.

[8] Katayama T, Imaizumi K, Honda A, Yoneda T, Kudo T, Takeda M, Mori K, Rozmahel R, Fraser P, George-Hyslop PS, Tohyama M (2001) Disturbed activation of endoplasmic reticulum stress transducers by familial Alzheimer's disease-linked presenilin-1 mutations. *J Biol Chem* **276**, 43446-43454.

[9] Hoozemans JJ, van Haastert ES, Eikelenboom P, de Vos RA, Rozemuller JM, Scheper W (2007) Activation of the unfolded protein response in Parkinson's disease. *Biochem Biophys Res Commun* **354**, 707-711.

[10] Zong WX, Li C, Hatzivassiliou G, Lindsten T, Yu QC, Yuan J, Thompson CB (2003) Bax and Bak can localize to the endoplasmic reticulum to initiate apoptosis. *J Cell Biol* **162**, 59-69.

[11] Urano F, Wang X, Bertolotti A, Zhang Y, Chung P, Harding HP, Ron D (2000) Coupling of stress in the ER to activation of JNK protein kinases by transmembrane protein kinase IRE1. *Science* **287**, 664-666.

[12] Rao RV, Castro-Obregon S, Frankowski H, Schuler M, Stoka V, del RG, Bredesen DE, Ellerby HM (2002) Coupling endoplasmic reticulum stress to the cell death program. An Apaf-1-independent intrinsic pathway. *J Biol Chem* **277**, 21836-21842.

[13] Kim HJ, Cho HK, Kwon YH (2008) Synergistic induction of ER stress by homocysteine and beta-amyloid in SH-SY5Y cells. *J Nutr Biochem* **19**, 754-761.

[14] Hoozemans JJ, van Haastert ES, Nijholt DA, Rozemuller AJ, Eikelenboom P, Scheper W (2009) The unfolded protein response is activated in pretangle neurons in Alzheimer's disease hippocampus. *Am J Pathol* **174**, 1241-1251.

[15] Hoozemans JJ, Veerhuis R, van Haastert ES, Rozemuller JM, Baas F, Eikelenboom P, Scheper W (2005) The unfolded protein response is activated in Alzheimer's disease. *Acta Neuropathol* **110**, 165-172.

[16] Hosoi T, Ozawa K (2010) Endoplasmic reticulum stress in disease: mechanisms and therapeutic opportunities. *Clin Sci (Lond)* **118**, 19-29.

[17] Terro F, Czech C, Esclaire F, Elyaman W, Yardin C, Baclet MC, Touchet N, Tremp G, Pradier L, Hugon J (2002) Neurons overexpressing mutant presenilin-1 are more sensitive to apoptosis induced by endoplasmic reticulum-Golgi stress. *J Neurosci Res* **69**, 530-539.

[18] Yu MS, Suen KC, Kwok NS, So KF, Hugon J, Chang RC (2006) Beta-amyloid peptides induces neuronal apoptosis via a mechanism independent of unfolded protein responses. *Apoptosis* **11**, 687-700.

[19] Lai CS, Preisler J, Baum L, Lee DH, Ng HK, Hugon J, So KF, Chang RC (2009) Low molecular weight Abeta induces collapse of endoplasmic reticulum. *Mol Cell Neurosci* **41**, 32-43.

[20] Spatara ML, Robinson AS (2010) Transgenic mouse and cell culture models demonstrate a lack of mechanistic connection between endoplasmic reticulum stress and tau dysfunction. *J Neurosci Res* **88**, 1951-1961.

[21] Ho YS, Yu MS, Yang XF, So KF, Yuen WH, Chang RCC (2010) Neuroprotective effects of polysaccharides from wolfberry, the fruits of Lycium barbarum, against homocysteine-induced toxicity in rat cortical neurons. *J Alzheimers Dis.* **19**, 813-827.

[22] Cheung YT, Zhang NQ, Hung CH, Lai CS, Yu MS, So KF, Chang RCC (2011) Temporal relationship of autophagy and apoptosis in neurons challenged by low molecular weight beta-amyloid peptide. *J.Cell Mol.Med* **15**, 244-257.

[23] Lewis J, McGowan E, Rockwood J, Melrose H, Nacharaju P, Van SM, Gwinn-Hardy K, Paul MM, Baker M, Yu X, Duff K, Hardy J, Corral A, Lin WL, Yen SH, Dickson DW, Davies P, Hutton M (2000) Neurofibrillary tangles, amyotrophy and progressive motor disturbance in mice expressing mutant (P301L) tau protein. *Nat Genet* **25**, 402-405.

[24] Sahara N, Lewis J, DeTure M, McGowan E, Dickson DW, Hutton M, Yen SH (2002) Assembly of tau in transgenic animals expressing P301L tau: alteration of phosphorylation and solubility. *J Neurochem* **83**, 1498-1508.

[25] Ho YS, Yu MS, Yik SY, So KF, Yuen WH, Chang RC (2009) Polysaccharides from wolfberry antagonizes glutamate excitotoxicity in rat cortical neurons. *Cell Mol Neurobiol* **29**, 1233-1244.

[26] Chang RCC, Yu MS, Lai CS (2006) Significance of molecular signaling for

protein translation control in neurodegenerative diseases. *Neurosignals* **15**, 249-258.

[27] Kins S, Crameri A, Evans DR, Hemmings BA, Nitsch RM, Gotz J (2001) Reduced protein phosphatase 2A activity induces hyperphosphorylation and altered compartmentalization of tau in transgenic mice. *J Biol Chem* **276**, 38193-38200.

[28] Kim D, Su J, Cotman CW (1999) Sequence of neurodegeneration and accumulation of phosphorylated tau in cultured neurons after okadaic acid treatment. *Brain Res* **839**, 253-262.

[29] Arendt T, Holzer M, Bruckner MK, Janke C, Gartner U (1998) The use of okadaic acid in vivo and the induction of molecular changes typical for Alzheimer's disease. *Neuroscience* **85**, 1337-1340.

[30] Vogel J, Anand VS, Ludwig B, Nawoschik S, Dunlop J, Braithwaite SP (2009) The JNK pathway amplifies and drives subcellular changes in tau phosphorylation. *Neuropharmacology* **57**, 539-550.

[31] Calfon M, Zeng H, Urano F, Till JH, Hubbard SR, Harding HP, Clark SG, Ron D (2002) IRE1 couples endoplasmic reticulum load to secretory capacity by processing the XBP-1 mRNA. *Nature* **415**, 92-96.

[32] Wang XZ, Lawson B, Brewer JW, Zinszner H, Sanjay A, Mi LJ, Boorstein R, Kreibich G, Hendershot LM, Ron D (1996) Signals from the stressed endoplasmic reticulum induce C/EBP-homologous protein (CHOP/GADD153). *Mol Cell Biol* **16**, 4273-4280.

[33] Takadera T, Fujibayashi M, Kaniyu H, Sakota N, Ohyashiki T (2007) Caspase-dependent apoptosis induced by thapsigargin was prevented by glycogen synthase kinase-3 inhibitors in cultured rat cortical neurons. *Neurochem Res* **32**, 1336-1342.

[34] Fasulo L, Ugolini G, Visintin M, Bradbury A, Brancolini C, Verzillo V, Novak M, Cattaneo A (2000) The neuronal microtubule-associated protein tau is a substrate for caspase-3 and an effector of apoptosis. *J Neurochem* **75**, 624-633.

[35] Yin H, Kuret J (2006) C-terminal truncation modulates both nucleation and extension phases of tau fibrillization. *FEBS Lett* **580**, 211-215.

[36] Ozcan U, Yilmaz E, Ozcan L, Furuhashi M, Vaillancourt E, Smith RO, Gorgun CZ, Hotamisligil GS (2006) Chemical chaperones reduce ER stress and restore glucose homeostasis in a mouse model of type 2 diabetes. *Science* **313**, 1137-1140.

[37] Sabala P, Czarny M, Woronczak JP, Baranska J (1993) Thapsigargin: potent inhibitor of Ca2+ transport ATP-ases of endoplasmic and sarcoplasmic reticulum. *Acta Biochim Pol* **40**, 309-319.

[38] Hartigan JA, Johnson GV (1999) Transient increases in intracellular calcium

result in prolonged site-selective increases in Tau phosphorylation through a glycogen synthase kinase 3beta-dependent pathway. *J Biol Chem* **274**, 21395-21401.

[39] Morgan D, Munireddy S, Alamed J, DeLeon J, Diamond DM, Bickford P, Hutton M, Lewis J, McGowan E, Gordon MN (2008) Apparent behavioral benefits of tau overexpression in P301L tau transgenic mice. *J Alzheimers Dis* **15**, 605-614.

[40] Arendash GW, Lewis J, Leighty RE, McGowan E, Cracchiolo JR, Hutton M, Garcia MF (2004) Multi-metric behavioral comparison of APPsw and P301L models for Alzheimer's disease: linkage of poorer cognitive performance to tau pathology in forebrain. *Brain Res* **1012**, 29-41.

[41] Ramsden M, Kotilinek L, Forster C, Paulson J, McGowan E, SantaCruz K, Guimaraes A, Yue M, Lewis J, Carlson G, Hutton M, Ashe KH (2005) Age-dependent neurofibrillary tangle formation, neuron loss, and memory impairment in a mouse model of human tauopathy (P301L). *J Neurosci* **25**, 10637-10647.

[42] Perreault S, Bousquet O, Lauzon M, Paiement J, Leclerc N (2009) Increased association between rough endoplasmic reticulum membranes and mitochondria in transgenic mice that express P301L tau. *J Neuropathol Exp Neurol* **68**, 503-514.

[43] Yoshiyama Y, Higuchi M, Zhang B, Huang SM, Iwata N, Saido TC, Maeda J, Suhara T, Trojanowski JQ, Lee VM (2007) Synapse loss and microglial activation precede tangles in a P301S tauopathy mouse model. *Neuron* **53**, 337-351.

[44] Kim SM, Yoon SY, Choi JE, Park JS, Choi JM, Nguyen T, Kim DH (2010) Activation of eukaryotic initiation factor-2 alpha-kinases in okadaic acid-treated neurons. *Neuroscience* **169**, 1831-1839.

[45] Yoon S, Choi J, Yoon J, Huh JW, Kim D (2006) Okadaic acid induces JNK activation, bim overexpression and mitochondrial dysfunction in cultured rat cortical neurons. *Neurosci Lett* **394**, 190-195.

[46] Kerokoski P, Suuronen T, Salminen A, Soininen H, Pirttila T (2001) The levels of cdk5 and p35 proteins and tau phosphorylation are reduced during neuronal apoptosis. *Biochem Biophys Res Commun* **280**, 998-1002.

[47] Rametti A, Esclaire F, Yardin C, Terro F (2004) Linking alterations in tau phosphorylation and cleavage during neuronal apoptosis. *J Biol Chem* **279**, 54518-54528.

[48] Linford NJ, Dorsa DM (2002) 17beta-Estradiol and the phytoestrogen genistein attenuate neuronal apoptosis induced by the endoplasmic reticulum calcium-ATPase inhibitor thapsigargin. *Steroids* **67**, 1029-1040.

[49] Nakagawa T, Zhu H, Morishima N, Li E, Xu J, Yankner BA, Yuan J (2000) Caspase-12 mediates endoplasmic-reticulum-specific apoptosis and

cytotoxicity by amyloid-beta. *Nature* **403**, 98-103.

[50] Fu ZQ, Yang Y, Song J, Jiang Q, Liu ZC, Wang Q, Zhu LQWJZ, Tian Q (2010) LiCl attenuates thapsigargin-induced tau hyperphosphorylation by inhibiting GSK-3beta in vivo and in vitro. *J Alzheimers Dis* **21**, 1107-1117.

[51] Sagara Y, Inesi G (1991) Inhibition of the sarcoplasmic reticulum Ca2+ transport ATPase by thapsigargin at subnanomolar concentrations. *J Biol Chem* **266**, 13503-13506.

[52] Matthews-Roberson TA, Quintanilla RA, Ding H, Johnson GV (2008) Immortalized cortical neurons expressing caspase-cleaved tau are sensitized to endoplasmic reticulum stress induced cell death. *Brain Res* **1234**, 206-212.

[53] Meske V, Albert F, Richter D, Schwarze J, Ohm TG (2003) Blockade of HMG-CoA reductase activity causes changes in microtubule-stabilizing protein tau via suppression of geranylgeranylpyrophosphate formation: implications for Alzheimer's disease. *Eur J Neurosci* **17**, 93-102.

[54] Saito T, Konno T, Hosokawa T, Asada A, Ishiguro K, Hisanaga S (2007) p25/cyclin-dependent kinase 5 promotes the progression of cell death in nucleus of endoplasmic reticulum-stressed neurons. *J Neurochem* **102**, 133-140.

[55] Ling ZQ, Tian Q, Wang L, Fu ZQ, Wang XC, Wang Q, Wang JZ (2009) Constant illumination induces Alzheimer-like damages with endoplasmic reticulum involvement and the protection of melatonin. *J Alzheimers Dis* **16**, 287-300.

[56] Althausen S, Paschen W (2000) Homocysteine-induced changes in mRNA levels of genes coding for cytoplasmic- and endoplasmic reticulum-resident stress proteins in neuronal cell cultures. *Brain Res Mol Brain Res* **84**, 32-40.

[57] Oida Y, Shimazawa M, Imaizumi K, Hara H (2008) Involvement of endoplasmic reticulum stress in the neuronal death induced by transient forebrain ischemia in gerbil. *Neuroscience* **151**, 111-119.

[58] Zhang CE, Tian Q, Wei W, Peng JH, Liu GP, Zhou XW, Wang Q, Wang DW, Wang JZ (2008) Homocysteine induces tau phosphorylation by inactivating protein phosphatase 2A in rat hippocampus. *Neurobiol Aging* **29**, 1654-1665.

[59] Wen Y, Yang S, Liu R, Simpkins JW (2004) Transient cerebral ischemia induces site-specific hyperphosphorylation of tau protein. *Brain Res* **1022**, 30-38.

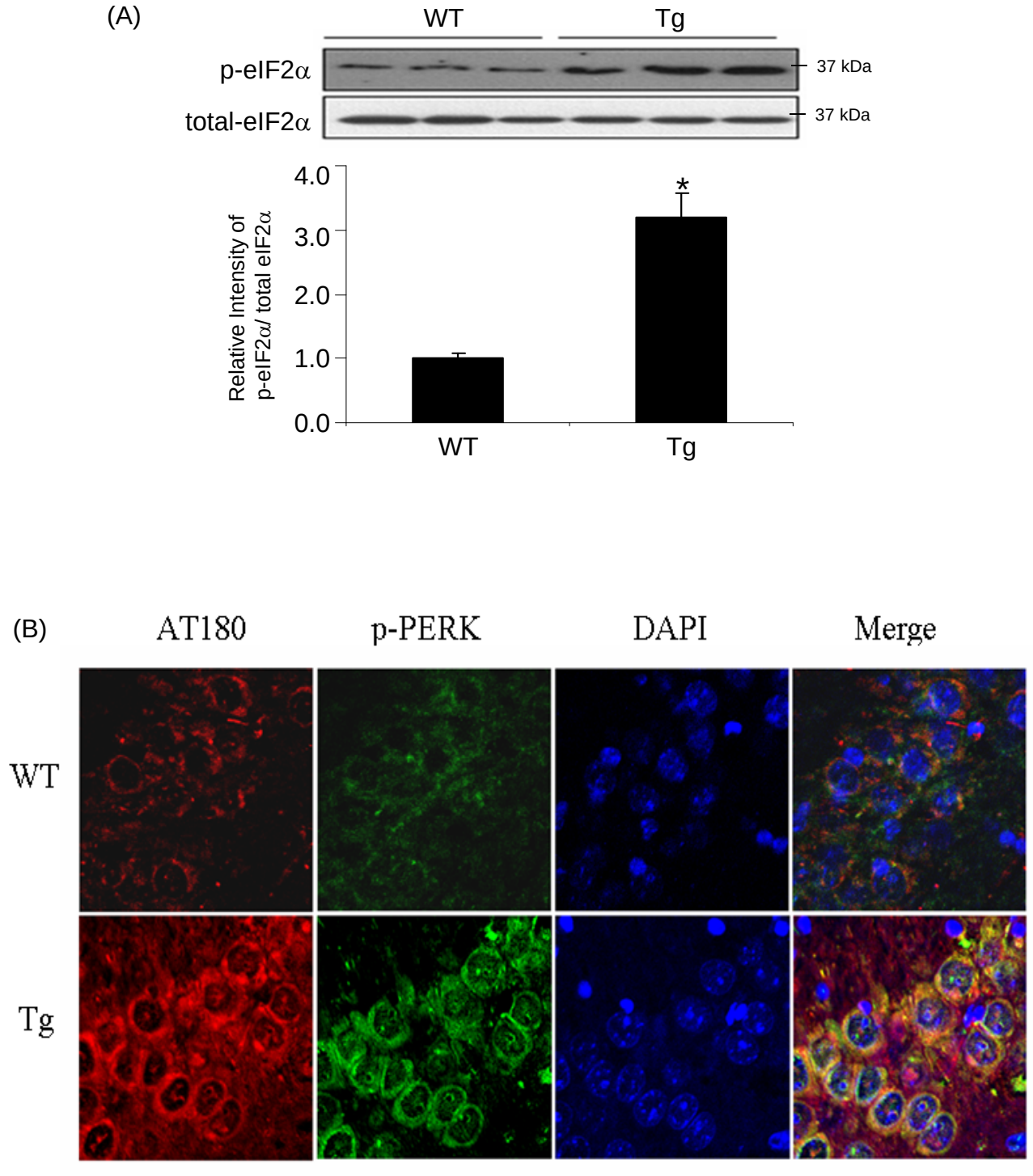

Fig. 1

Ho *et. al.*, 2011

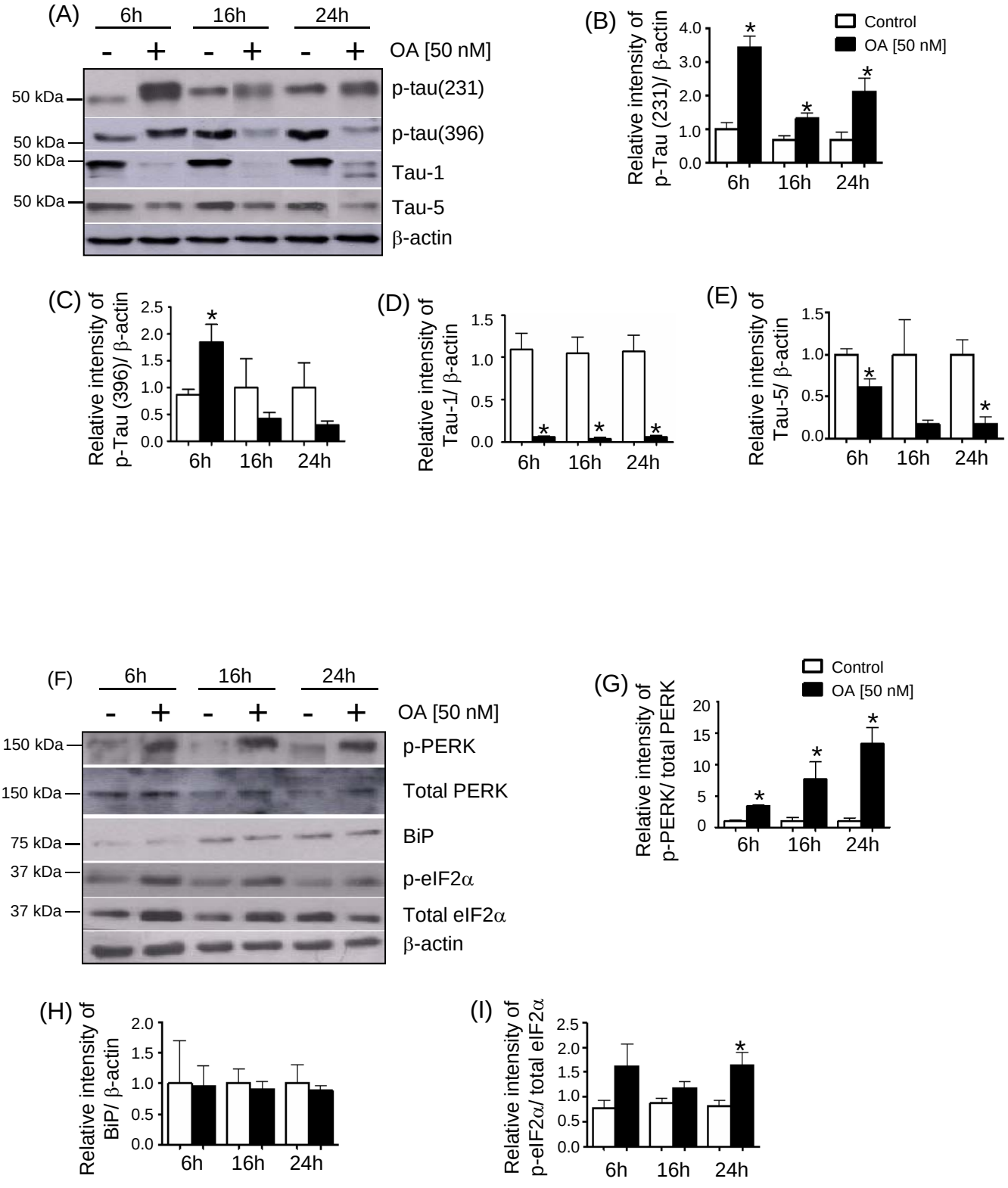

Fig. 2

Ho *et. al.*, 2011

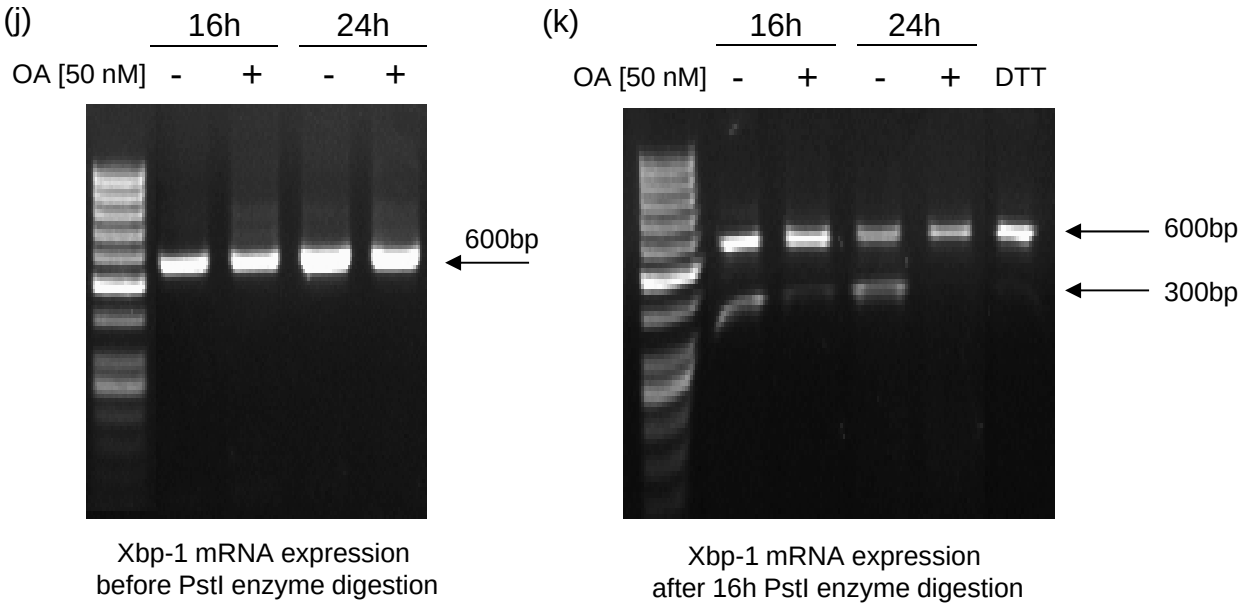

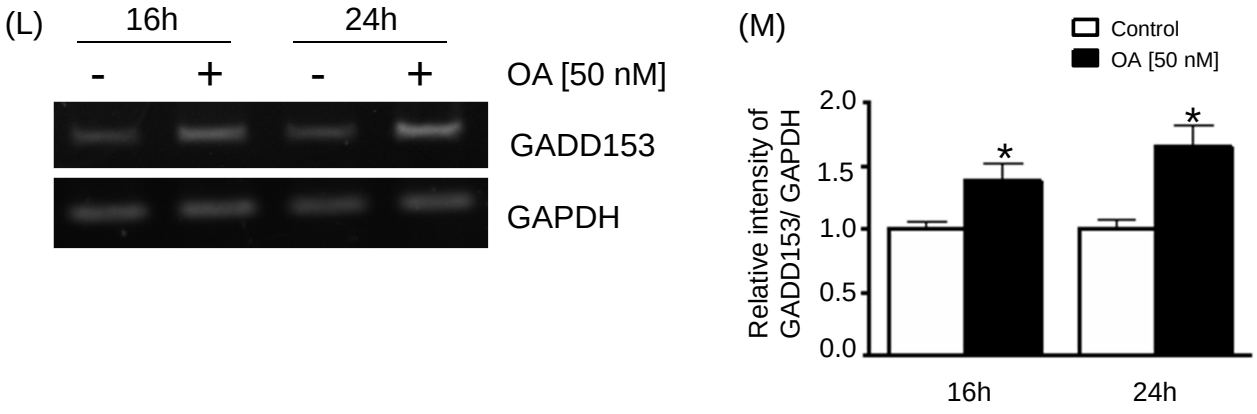

Fig. 2

Ho *et. al.*, 2011

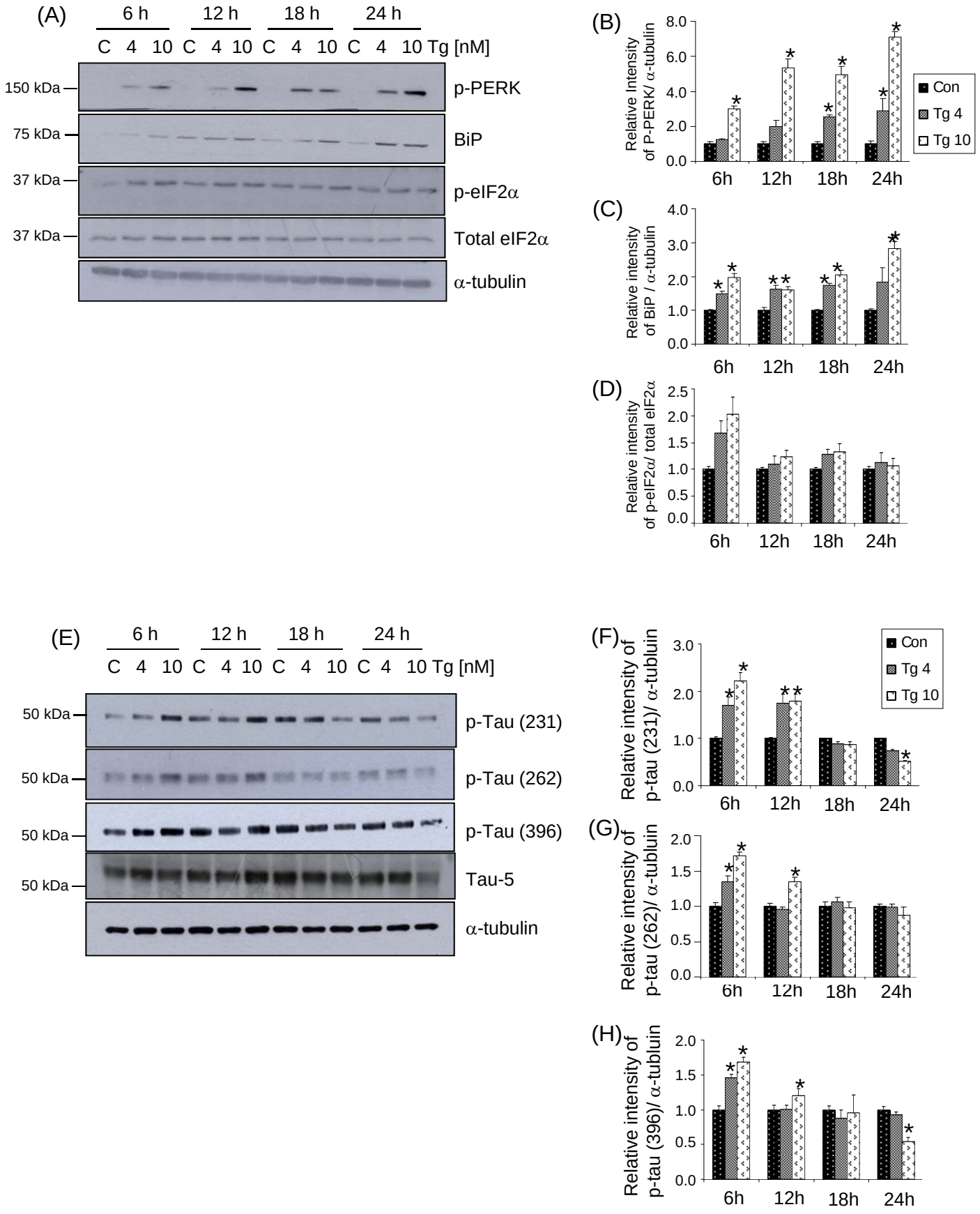

Fig. 3

Ho *et. al.*, 2011

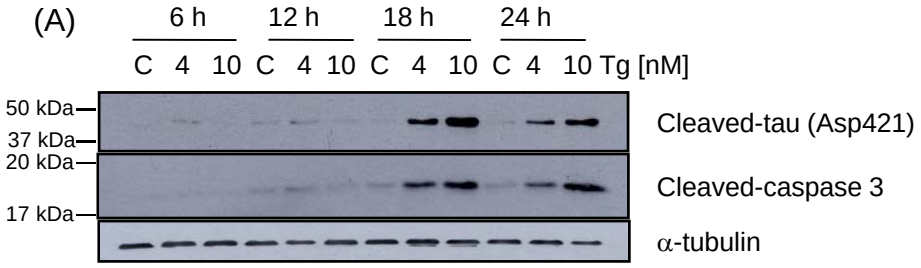

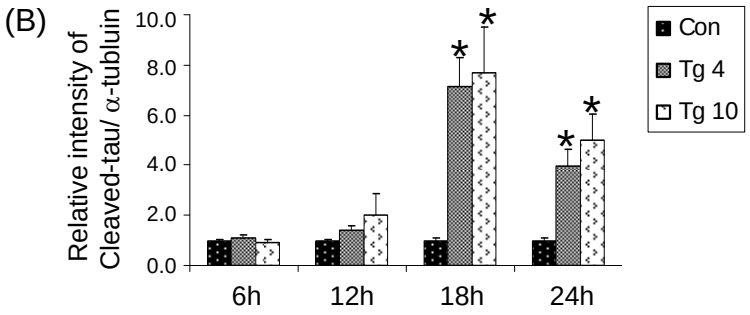

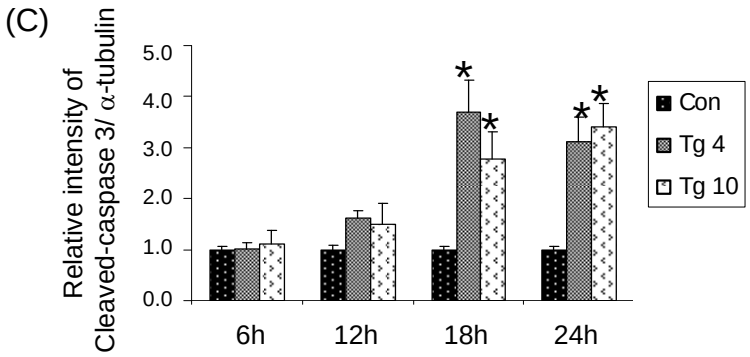

Fig. 4

Ho *et. al.*, 2011

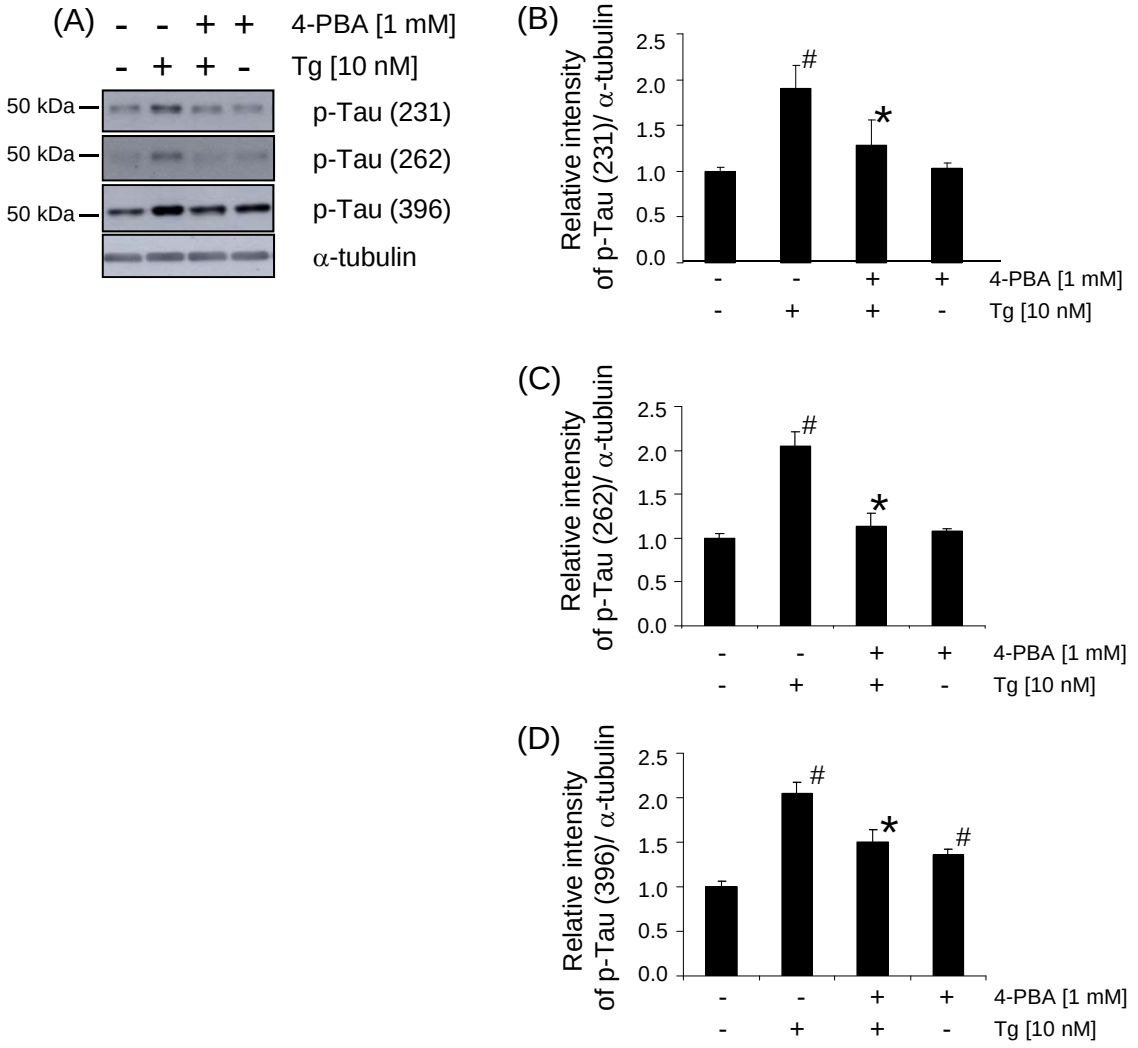

Fig. 5

Ho *et. al.*, 2011

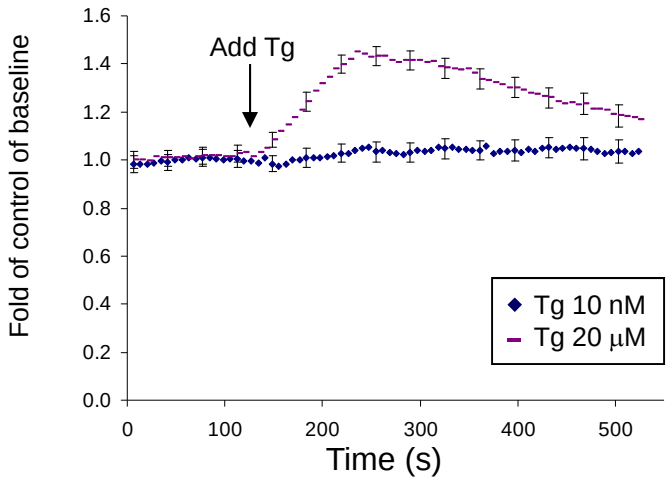

Fig. 6

Ho *et. al.*, 2011

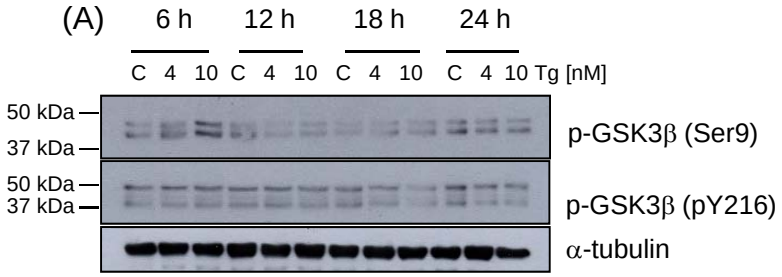

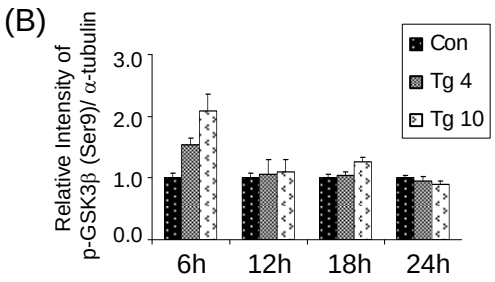

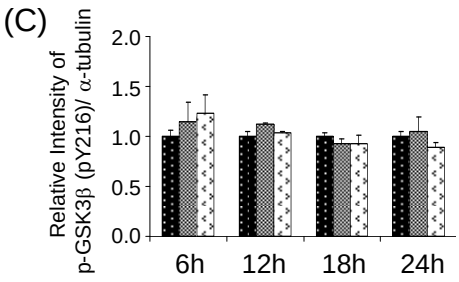

Fig. 7

Ho *et. al.*, 2011

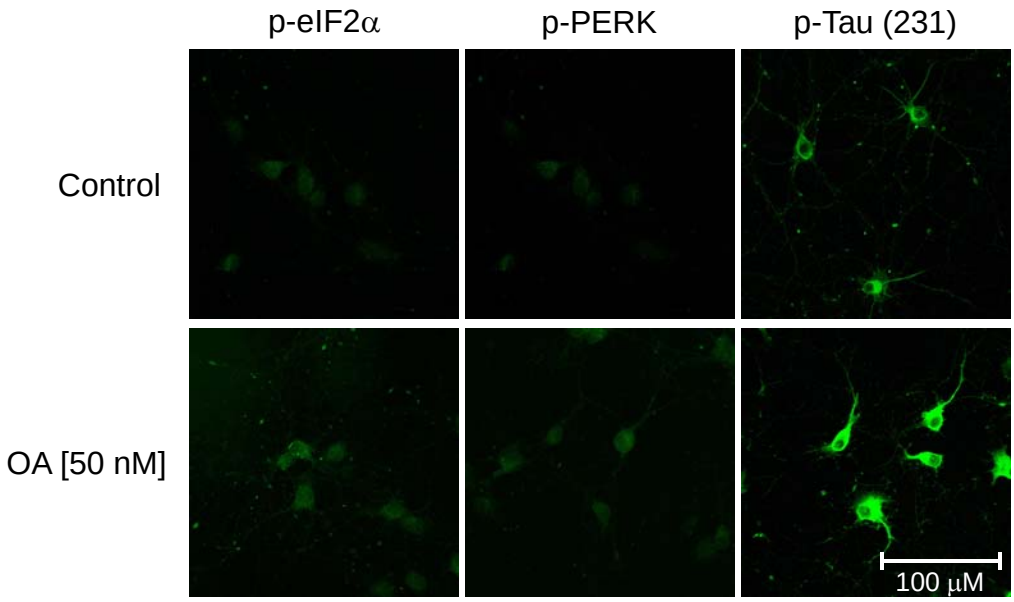

Supplementary Fig.1 OA-induced hyperphosphorylation of tau led to ER-stress in primary cultures of hippocampal neurons. OA [50 nM] was added to neuronal cultures and incubated for 6h to induce tau hyperphosphorylation. The neurons were fixed with 4% paraformaldehyde and stained with specific antibodies against p-Tau (231), p-Tau (396), Tau 5 and p-PERK. Representative photos of each group are shown, magnification = 40X. The level of p-Tau (231) was markedly increased in the OA-treated group. In the same time, the levels of p-eIF2a A and p-PERK were also increased.

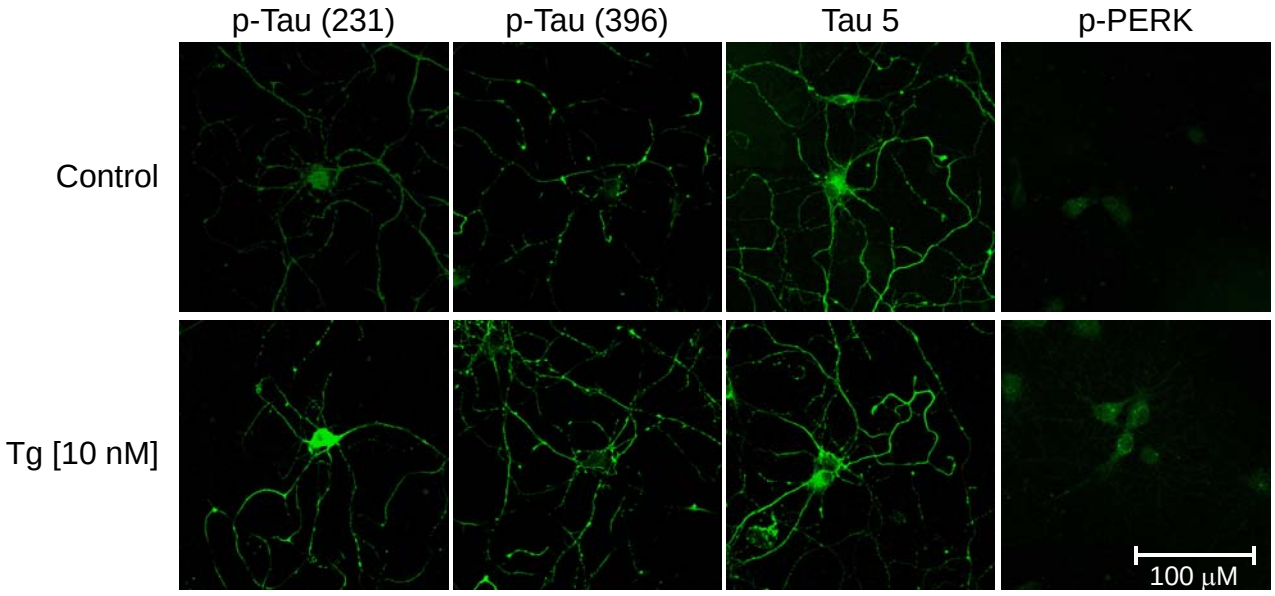

Supplementary Fig.2 Tg induced UPR and phosphorylation of tau in primary cultures of hippocampal neurons. Tg [10 nM] was added to neuronal cultures and incubated for 6h to induce ER-stress. The neurons were fixed with 4% paraformaldehyde and stained with specific antibodies against p-Tau (231), p-Tau (396), Tau 5 and p-PERK. Representative photos of each group are shown, magnification = 40X. The level of p-PERK, a UPR marker, was elevated in the Tg-treated group. In the same time, the levels of p-Tau (231), p-Tau (396) were also increased. The level of total tau, which detected by the Tau 5 antibody remained unchanged.

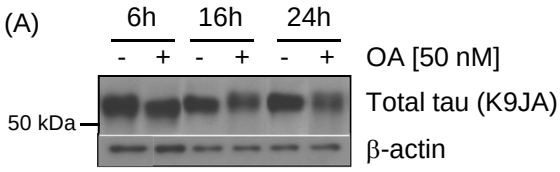

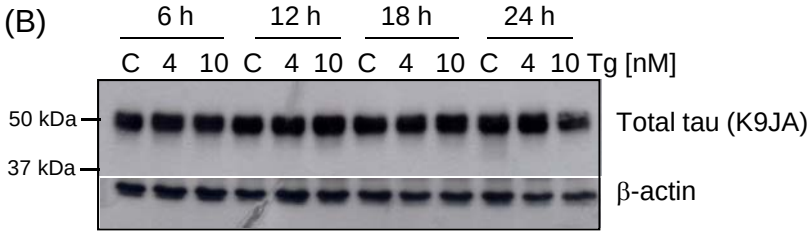

Supplementary Fig.3 Levels of total tau were further confirmed by using the Tau-5 antibody. (A) The pattern of total tau detected by Tau-5 antibody in OA-treated cultures was similar to those detected by the K9JA pan-tau antibody in Fig. 2A. (B) The pattern of total tau detected by Tau-5 antibody in Tg-treated cultures was similar to those detected by the K9JA pan-tau antibody in Fig. 3E.